Hindawi
Shock and Vibration
Volume 2023, Article ID 9524177, 19 pages
https://doi.org/10.1155/2023/9524177

Research Article

Investigating Fractional Damping Effect on Euler–Bernoulli Beam Subjected to a Moving Load

Raed AlSaleh,[1] **Ayman Nasir**,[2] **and Ibrahim Abu-Alshaikh**[2,3]

[1]*German Jordanian University, Amman, Jordan*
[2]*Al-Zaytoonah University of Jordan, Amman, Jordan*
[3]*The University of Jordan, Amman, Jordan*

Correspondence should be addressed to Raed AlSaleh; raed.alsaleh@gju.edu.jo

Received 14 March 2023; Revised 24 May 2023; Accepted 7 June 2023; Published 20 June 2023

Academic Editor: Abdollah Malekjafarian

In this work, the dynamic response of Euler–Bernoulli beams of four different boundary conditions with fractional order internal damping under a traversing moving load is investigated. The load is assumed to be moving with different values of constant velocity. A proposed approach to obtain the closed-form solution of the problem based on Green's functions combined with a decomposition technique in the Laplace transform domain is introduced. Several cases are studied and compared to the literature; for instance, if simply supported beam is considered, the following three cases are to be explored: the case of elastic (or undamped) beam, the damped (or viscously damped) beam, and finally the fractionally damped beam modeled by the fractional Kelvin–Voigt model. The effects to the beam dynamic response induced by magnitude of moving load velocity, damping ratio, and fractional damping order are explored. The results expressed sufficient agreement with similar problems found in literature and evidenced that the dynamic response of beams is significantly affected by varying the fractional order of beam damping as well as the moving load velocity. Accordingly, using fractionally damped materials exhibits better realistic behavior of beams and intermediate between elastic and viscous beam behaviors.

1. Introduction

The subject of dynamic response under diverse types of loading for beams of viscoelastic materials is considered of utmost importance. Many applications of beams are found in bridges, railways, aircraft, and vehicles. As a result, various progressive studies have been performed to address the damping conduct of such materials (Rossikhin et al. [1], Paunović et al. [2], and Klanner et al. [3]).

The prevalent use of the Euler–Bernoulli beam model is attributed to its simplicity and ability to give reasonable estimations for various engineering issues. Utilizing the Euler–Bernoulli's equation, Hilal and Zibdeh [4] presented a paper contributory to the major issue concerning the vibrations of an elastic homogenous isotropic beam excited by moving loads under generic boundary conditions. The beam was subjected to moving force with constant velocity and according to the beam's response; closed-form solutions were acquired. In this study, Sumelka et al. [5] reformulated the classical Euler–Bernoulli theory utilizing fractional calculus. Such generalization was called fractional Euler–Bernoulli beams, and it resulted in nonlocal spatial description. After two years, Blaszczyk [6] derived the Euler–Bernoulli beam equation by using the variational approach that leads the equation to contain left and right fractional Caputo derivatives simultaneously. Then, it was transformed into an integral equation to be solved analytically and numerically.

On the other hand, Fractional derivative models have proven to be of significant value for the precise characterization of the damping behavior of various types of materials (Bagley and Torvik [7]). Leibnitz and De L'Hospital were the first to have introduced the concept of fractional derivatives in the 16th century (Podlubny [8]). When compared to different mathematical models including the Maxwell model, Kelvin–Voigt model, or other models instituted by

Flügge [9], Pipkin [10], and Christensen [11], the fractional derivative model was found to coincide with the experimental data very well utilizing fewer parameters according to Di Paola et al. [12]. Thus, studying the damping properties of materials using these techniques is becoming essential and proven to be efficacious.

Adolfsson [13] used the fractional order model in investigations involving viscoelastic materials to obtain the large deformations of investigated beams. Studies on the dynamic response of beams resting on fractional viscoelastic foundation are also found in the literature. The effect of the moving load velocity on such beams was presented by Ouzizi et al. [14], while the same authors investigated the effect of inducing multiple harmonic moving loads with a constant speed on the beam dynamical response (Ouzizi et al. [15]). More recently, in the study by Praharaj and Datta [16], the same beam response was investigated again when subjected to a moving load. In this study, the fractional order derivative-based Kelvin–Voigt model was used to describe the rheological properties of the viscoelastic foundation, while the Reimann–Liouville fractional derivative model was applied for a fractional derivative order, and the resulted fractional differential equation of motion was solved by applying the modal superposition method and triangular strip matrix approach. In all of these studies, the effects of different system parameters on the beam response were evaluated.

The solution of a fractionally damped beam equation is examined by Jena et al. [17] by applying the homotopy analysis method to calculate the dynamic response. The unit step and unit impulse functions are deliberated for this analysis, and the acquired results for different orders of the fractional derivatives are compared well with others and achieved by the Adomian decomposition method, which was used in 2007 by Liang and Tang [18] to derive the analytical solution of viscoelastic that continues fractionally damped beam considering step and impulse function responses.

In 2016, a study involving a nonproportionally damped Euler–Bernoulli beam, which was subjected to moving loads, determined an analytical solution to assess the dynamic properties of such systems (Svedholm et al. [19]). In this investigation, it was assumed that the system's dynamic behavior can be assessed by superposition considering that adequate orthogonality conditions were derived and a closed-form solution for the dynamic behavior for a given eigenvalue was proposed. In the same year, Freundlich adopted the modal superposition approach to obtain the solution for force vibrations of a fractionally damped beam, while a convolution integral of fractional forcing function and Green's function were utilized to acquire the beam's behavior. Then, an assessment of the beam's dynamic response under different fractional derivative orders and the moving load's velocities was performed. Green's function model was also used back in 1997 by Foda and Abduljabbar to investigate the effects of various parameters on the dynamic behavior of a plainly propped Euler– Bernoulli beam submitted under a transverse moving load. The process was then proven to be simple and effective.

In this study, Labędzki et al. [20] modeled both stiffness and damping terms in the Euler–Bernoulli beam equations using fractional derivatives for the Cantilever case this time. The equations were formulated and solved for beams with and without tip mass. The other two boundary conditions (namely, fixed-fixed and Cantilever-fixed) were considered by Blaszczyk et al. [21] to be analyzed by the fractional Euler–Bernoulli beam equation, where the differential equation of motion was converted into an integral one considering the mentioned boundary conditions and exact solution was obtained, which contained a composition of the left and right Reimann–Liouville integrals. The study presented three solutions for a constant, power, and trigonometric functions. On the other hand, Abro et al. [22] presented an analytic study of a simply supported beam case based on the modern fractional approaches utilizing Caputo–Fabrizio and Atanagna–Baleanu fractional differential operators. The equation of motion was fractionalized to investigate the effects of principal parametric resonances, and Laplace and Fourier sine transforms were invoked for investigating the exact solution.

Considering that the fractional derivative provides reliable models of fractionally damped structures and that few contributions have been introduced in this field so far, the need is still there to realize more generic closed-form solutions and investigate the impact of different parametric changes on beams' response under different loading scenarios. Within this context, this study introduces a novel formulation of the closed-form solution of the Euler–Bernoulli beam with internal damping expressed by the fractional derivative, when traversed by a concentrated load moving with constant velocity, while considering the following four beam boundary conditions (BCs): pinned-pinned (PP), fixed-fixed (FF), fixed-pinned (FP), and fixed-free or Cantilever (FC). In the introduced approach, the governing equation of the Euler–Bernoulli beam described using the fractional Kelvin–Voigt model is written as a fourth order partial differential equation and Caputo's definition is employed for the fractional derivative. The orthogonality conditions are introduced to convert the partial differential equation into a second order ordinary differential equation, while at this stage, Laplace transform is exercised using the decomposition technique introduced in the study of Abu-Alshaikh et al. [23], combined with Green's theorem to obtain the closed-form solution of the problem.

For verification purposes, the obtained closed-form solution of the fractionally damped beam is utilized to obtain solutions for the beam without damping, and with integer order damping cases, these solutions are then compared with those available in the literature.

To conclude, the dynamic response of the fractionally damped Euler–Bernoulli beam having four different beam BCs (namely, pinned-pinned (PP), fixed-fixed (FF), fixed-pinned (FP), and fixed-free or Cantilever (FC)) is investigated in this paper. The analysis is based on Green's functions' approach combined with a decomposition technique in the Laplace transform domain; the closed-form solutions are analytically generated, and the results are discussed through the selected numerical examples.

Furthermore, the impacts bestowed upon the beams' response by the moving load velocity, damping ratio, and the order of fractional derivatives are illustrated. It is worth mentioning that all the obtained solutions are truncated using the mathematical software Maple (Maplesoft [24]). The resulted fractional derivative damping models may allow researchers to choose more suitable models to precisely fit experimental ones.

2. Basic Concepts and Formulations

The fundamental concepts of a beam model with fractional damping are introduced in this section. Primarily, detailed presentation of the basic formulation for the fractional Euler Bernoulli beam is shown using the fractional Kelvin–Voigt model. This is followed by a step-by-step solution of the equation of motion for different case studies deploying relations for internal damping of viscoelastic materials and natural frequencies of vibration modes for elastic beams, the generalized Delta function, fractional calculus, Green's functions, and some other special functions' concepts.

In order to study the beam with the fractional model of internal damping, the elastic behavior of the material should be studied with the aid of the Kelvin–Voigt model for creep, (Christensen [11]), which reveals the relation between the stress $\sigma(t)$ and strain $\varepsilon(t)$ in the elastic region, and since the strain rate, $\dot{\varepsilon}(t)$, is appearing in that model, it is possible to implement the theory of the fractional order derivatives to write the stress variations with time for any value of the fractional derivative, α, and its value in our work is $0 < \alpha \leq 1$. According to the fractional order Kelvin–Voigt model, which was proposed by Shermergor [25] and adopted in several following works, for instance, Rossikhin and Shitikova [26], and with further manipulations related to the derivation of this model, as in the study by Nasir [27], it is convenient to write the following:

$$\sigma(t) = E\varepsilon(t) + C_\alpha\left(D_0^\alpha(\varepsilon(t))\right) = E\varepsilon(t) + \frac{C_\alpha}{\Gamma(1-\alpha)}\int_0^t \frac{\dot{\varepsilon}(\tau)}{(t-\tau)^\alpha}\,\mathrm{d}\tau, \tag{1}$$

where E is the modulus of elasticity, μ is the viscous damping coefficient of the beam, C_α is the characteristic internal damping coefficient of the material, and $\Gamma(.)$ is Euler's Gamma function. Moreover, Caputo's definition of the fractional derivative, Podlubny [8], is used to write the fractional derivative in the integral form, and it is going to be used in this work to solve the beam's fractional order equation of motion, as will be discussed during the analysis.

After this brief discussion, as equation (1) illustrates, it can be found that one simple fractional model, the Kelvin–Voigt fractional model, can be applied for investigating the dynamics of viscoelastic materials, and this model has an intermediate behavior between elastic and viscous materials. For more discussion regarding this model and its applications, the interested reader is advised to visit (Bonfanti et al. [28]) and references therein.

Based on the aforementioned analysis, the governing equation of the Euler–Bernoulli beam described using the fractional Kelvin–Voigt model can be written as a fourth order partial differential equation (Di Lorenzo et al. [29]) in the form as follows:

$$\rho\frac{\partial^2 w(x,t)}{\partial t^2} + EI\left[\frac{\partial^4 w(x,t)}{\partial x^4}\right] + C_\alpha I\left[D_{0^+}^\alpha\left(\frac{\partial^4 w(x,t)}{\partial x^4}\right)\right] = mg\delta(x-vt), \tag{2}$$

where $w(x,t)$ is the transverse displacement of the neutral beam axis at point with coordinate x and time t, m is the moving load, which has a constant velocity v, and the term $\delta(x-vt)$ represents the Dirac delta function, which has a unity magnitude when $x = vt$; otherwise, it is equal to zero. Moreover, the term $D_{0^+}^\alpha(w(x,t)) = (\partial^\alpha w(x,t)/\partial t^\alpha)$ represents the fractional derivative of order α. This term is commonly introduced in the literature using various definitions; one of the most well-known definitions is the Caputo fractional derivative, Podlubny [8], which can be written as follows:

$$\frac{\partial^\alpha w(x,t)}{\partial t^\alpha} = \frac{1}{\Gamma(k-\alpha)}\int_0^t \frac{w(x,u)}{(t-u)^{\alpha+1-k}}\frac{\partial^k w(x,u)}{\partial u^k}\,\mathrm{d}u. \tag{3}$$

The model of equation (2) is a general representation of viscoelastic Euler–Bernoulli beams that can have various BCs, and this model is used to solve the problem under consideration for various beam end conditions: the pinned-pinned, fixed-fixed, pinned-fixed, and fixed-free cases, and different values of α between zero and unity are to be considered. In obtaining the solution for equation (2), the density ρ, modulus of elasticity E, moment of inertia I, and the characteristic coefficient of the material C_α are all assumed to be constants.

For any vibration mode, $\varphi_n(x)$ is considered, while $Y_n(t)$ is the vibration mode of the beam, the modal form of $w(x,t)$ can be written in the form of infinite series as follows:

$$w(x,t) = \sum_{n=1}^{\infty}\varphi_n(x)Y_n(t). \tag{4}$$

In equation (4), the subscript n denotes the mode number investigated, and the accuracy of the results depends on the total number of modes truncated using the series;

only the first mode of vibration is truncated in this work for which acceptable levels of accuracy are obtained. This is going to be discussed in detail during this analysis. Nevertheless, the theoretical procedure implemented enables the researcher, if desired, to effectively investigate a greater number of modes.

The undamped free vibration mode $\varphi_n(x)$ is written for general beam boundary condition as follows:

$$\varphi_n(x) = \sin(\gamma_n x) + A_n \cos(\gamma_n x) + B_n \sin h(\gamma_n x) + C_n \cos h(\gamma_n x), \tag{5}$$

where A_n, B_n, and C_n are constants evaluated from the BCs and γ_n is the root of the frequency equation, and all are obtained as listed in Table 1.

When substituting equations (4) into (2) and considering that $C_\alpha = E(\mu/E)^\alpha$, we get the following:

$$EI \sum_{n=1}^{N} \varphi_n^{iv}(x) Y_n(t) + C^\alpha I \sum_{n=1}^{N} \frac{d^\alpha Y_n(t)}{dt^\alpha} \varphi_n^{iv}(x) + \mu \sum_{n=1}^{N} \varphi_n(x) \ddot{Y}_n(t) = mg\delta(x - vt). \tag{6}$$

Multiplying each term by $\varphi_m(x)$ and integrating over the entire length of the beam from 0 to L gives the following:

$$\begin{aligned} &\int_0^L EI \sum_{n=1}^{N} \varphi_m(x) \varphi_n^{iv}(x) Y_n(t)\, dx + \int_0^L C^\alpha I \sum_{n=1}^{N} \frac{d^\alpha Y_n(t)}{dt^\alpha} \varphi_m(x) \varphi_n^{iv}(x) dx + \int_0^L \mu \sum_{n=1}^{N} \varphi_m(x)\, \varphi_n(x)\, \ddot{Y}_n(t) dx \\ &= \int_0^L mg \varphi_m(x) \delta(x - vt)\, dx, \end{aligned} \tag{7}$$

Now, it is possible to apply the orthogonality conditions, which imply the following important results:

$$\chi_n = \int_0^L \mu\, \varphi_n^2(x)\, dx, \tag{8}$$

$$\int_0^L \varphi_m(x)\, \varphi_n^{(iv)}(x)\, dx = \gamma_n^4 \begin{cases} 0, & if\ m \neq n, \\ \dfrac{\chi_n}{\mu}, & if\ m = n. \end{cases} \tag{9}$$

Using trigonometric and hyperbolic integration relations, it is simply shown that equation (9) is applicable for any combination of BCs (Rao [30]). Thus, in terms of equations (8) and (9), (7) becomes

$$EI \sum_{n=1}^{N} \gamma_n^4 Y_n(t) + C^\alpha I \sum_{n=1}^{N} \gamma_n^4 \frac{d^\alpha Y_n(t)}{dt^\alpha} + \mu \sum_{n=1}^{N} \ddot{Y}_n(t) \int_0^L \varphi_n^2(x) dx = mg \sum_{n=1}^{N} \int_0^L \varphi_n(x) \delta(x - vt) dx. \tag{10}$$

Let $P_0 = mg$, then the differential equation of the n^{th} mode of vibration of the generalized displacement or modal response of the beam may be rearranged and written as follows:

$$\begin{aligned} &EI \frac{\gamma_n^4 \chi_n}{\mu} Y_n(t) + C^\alpha I \frac{\gamma_n^4 \chi_n}{\mu} \frac{d^\alpha Y_n(t)}{dt^\alpha} + \chi_n \ddot{Y}_n(t) \\ &= P_0 \sum_{n=1}^{N} \phi_n(vt), \end{aligned} \tag{11}$$

or

$$\ddot{Y}_n(t) + \frac{C^\alpha I}{\mu} \gamma_n^4 \frac{d^\alpha Y_n(t)}{dt^\alpha} + \frac{EI}{\mu} \gamma_n^4 Y_n(t) = \frac{P_0}{\chi_n} \sum_{n=1}^{N} \varphi_n(vt). \tag{12}$$

Then, equation (12) can be solved using a decomposition method similar to that used in the study of Abu-Mallouh et al. [31] for a linear beam equation of motion; nevertheless, if the equation of motion is nonlinear, the same decomposition is

Table 1: Frequency equations and vibration modes for the transverse vibration of beams (Rao [30]).

Beam end conditions	Frequency equation	Vibration mode (normal function)	Value of $\beta_n l$
PP	$\sin(\gamma_n l) = 0$	$\phi_n(x) = C_n[\sin(\gamma_n x)]$	$\gamma_1 l = \pi$, $\gamma_2 l = 2\pi$ $\gamma_3 l = 3\pi$ $\gamma_4 l = 4\pi$
FF	$\cos(\gamma_n l)\cosh(\gamma_n l) = 1$	$\phi_n(x) = C_n\left\{\begin{matrix}\sin h(\gamma_n x) - \sin(\gamma_n x) \\ +\alpha_n[\cos h(\gamma_n x) - \cos(\gamma_n x)]\end{matrix}\right\}$ where $\alpha_n = (\sin h(\gamma_n l) - \sin(\gamma_n l))/(\cos(\gamma_n l) - \cos h(\gamma_n l))$	$\gamma_1 l = 4.730041$ $\gamma_2 l = 7.853205$ $\gamma_3 l = 10.99560$ $\gamma_4 l = 14.13765$
FP	$\tan(\gamma_n l)\tanh(\gamma_n l) = 0$	$\phi_n(x) = C_n\left\{\begin{matrix}\sin(\gamma_n x) - \sinh(\gamma_n x) \\ +\alpha_n[\cosh(\gamma_n x) - \cos(\gamma_n x)]\end{matrix}\right\}$ where $\alpha_n = (-\sin(\gamma_n l) - \sin(\gamma_n l))/(\cos(\gamma_n l) - \cosh(\gamma_n l))$	$\gamma_1 l = 3.926602$ $\gamma_2 l = 7.068583$ $\gamma_3 l = 10.21017$ $\gamma_4 l = 13.35177$
FC	$\cos(\gamma_n l)\cos h(\gamma_n l) = -1$	$\phi_n(x) = C_n\left\{\begin{matrix}\sin(\gamma_n x) - \sin h(\gamma_n x) \\ -\alpha_n[\cos(\gamma_n x) - \cos h(\gamma_n x)]\end{matrix}\right\}$ where $\alpha_n = \sin(\gamma_n l) + \sin(\gamma_n l)/\cos(\gamma_n l) + \cos h(\gamma_n l)$	$\gamma_1 l = 1.87504$ $\gamma_2 l = 4.69409$ $\gamma_3 l = 7.85457$ $\gamma_4 l = 10.9955$

primarily used and then another decomposition is applied to resolve the nonlinear terms; this process is normally called the Adomian decomposition method (ADM) for nonlinear systems, refer to Kwong et al. [32] for more details regarding the ADM and its applications. From equation (12), the solution of the vibration mode of the beam, $Y_n(t)$, is assumed to have a series form as follows:

$$Y_n(t) = \sum_{J=0}^{\infty} Y_n^J(t). \tag{13}$$

So, equation (12), in view of equation (13), is written as follows:

$$\sum_{J=0}^{\infty} \ddot{Y}_n^J(t) + \frac{C^\alpha I \gamma_n^4}{\mu} \sum_{J=0}^{\infty} \frac{\mathrm{d}^\alpha Y_n^J(t)}{\mathrm{d}t^\alpha} + \frac{EI\gamma_n^4}{\mu} \sum_{J=0}^{\infty} Y_n^J(t) = \frac{P_0}{\chi_n} \sum_{n=1}^{N} \varphi_n(vt). \tag{14}$$

Substituting the n^{th} natural frequency ω_n and the damping ratio ζ_n as follows:

$$\omega_n = \gamma_n^2 \sqrt{\frac{EI}{\mu}}, \qquad \zeta_n = \frac{C^\alpha I \gamma_n^4}{2\mu\omega_n} = \frac{C^\alpha \omega_n}{2E}. \tag{15}$$

Thus, equation (14) becomes

$$\sum_{J=0}^{\infty} \ddot{Y}_n^J(t) + 2\omega_n\zeta_n \sum_{J=0}^{\infty} \frac{\mathrm{d}^\alpha Y_n^J(t)}{\mathrm{d}t^\alpha} + \omega_n^2 \sum_{J=0}^{\infty} Y_n^J(t) = \frac{P_0}{\chi_n} \sum_{n=1}^{N} \varphi_n(vt), \tag{16}$$

and by rearranging equation (16), we get the following:

$$\sum_{J=0}^{\infty} \ddot{Y}_n^J(t) + \omega_n^2 \sum_{J=0}^{\infty} Y_n^J(t) = \frac{P_0}{\chi_n} \sum_{n=1}^{N} \varphi_n(vt) - 2\omega_n\zeta_n \sum_{J=0}^{\infty} \frac{\mathrm{d}^\alpha Y_n^J(t)}{\mathrm{d}t^\alpha}. \tag{17}$$

Applying the decomposition form illustrated in equation (13), equation (17) can be divided into a system of two recursive equations as follows:

$$\frac{\mathrm{d}^2 Y_n^0(t)}{\mathrm{d}t^2} + \omega_n^2 Y_n^0(t) = \frac{P_0}{\chi_n}\varphi_n(\nu t), \tag{18}$$

$$\frac{\mathrm{d}^2 Y_n^J(t)}{\mathrm{d}t^2} + \omega_n^2 Y_n^J(t) = -2\omega_n\zeta_n \frac{\mathrm{d}^\alpha Y_n^{J-1}(t)}{\mathrm{d}t^\alpha}\ ;\ J \geq 1. \tag{19}$$

It is noteworthy that in equation (18), the subscript n denotes the vibration mode to be studied, while in equation (19), the superscript J is used to indicate the number of terms considered in the decomposition. In the following equations, for enhanced readability, the summation signs in equations (18) and (19) are dropped (same for the following equations); nevertheless, when writing the final solutions, the summation terms are to be reconsidered. Now, by defining $\Phi_n(s)$ to be the Laplace transform of the vibration mode function, as shown in equation (5), then we get the following:

$$\Phi_n(s) = \frac{\Omega_n}{s^2+\Omega_n^2} + \frac{A_n s}{s^2+\Omega_n^2} + \frac{B_n\Omega_n}{s^2-\Omega_n^2} + \frac{C_n s}{s^2-\Omega_n^2}, \tag{20}$$

where $\Omega_n = \gamma_n \nu$. Taking the Laplace transform for equation (18), while assuming homogenous conditions, yields to the following:

$$s^2 y_n^0(s) + \omega_n^2 y_n^0(s) = \frac{P_0}{\chi_n}\Phi_n(s). \tag{21}$$

Then, the initial part of the solution in the Laplace domain is simplified by rearranging equation (21) in terms of $y_n^0(s)$ and then applying the direct Laplace inverse to get the initial solution in the time domain denoted by $Y_n^0(t)$, as follows:

$$Y_n^0(t) = \frac{P_0}{\chi_n\omega_{\mathrm{n}}^2\left(\Omega_n^4-\omega_{\mathrm{n}}^4\right)}\left\{\begin{array}{c} -\left(\Omega_n^2+\omega_{\mathrm{n}}^2\right)\left[\Omega_n i\omega_n \sin \mathrm{h}\left(i\omega_n t\right) + \omega_{\mathrm{n}}^2 \sin\left(\Omega_n t\right)\right] \\ + A_n\omega_{\mathrm{n}}^2\left(\Omega_n^2+\omega_{\mathrm{n}}^2\right)\left[\cos \mathrm{h}\left(i\omega_n t\right) - \cos\left(\Omega_n t\right)\right] \\ + B_n\left(\Omega_n^2-\omega_{\mathrm{n}}^2\right)\left[\Omega_n i\omega_n \sin \mathrm{h}\left(i\omega_n t\right) + \omega_{\mathrm{n}}^2 \sin \mathrm{h}\left(\Omega_n t\right)\right] \\ -A_n\omega_{\mathrm{n}}^2\left(\Omega_n^2-\omega_{\mathrm{n}}^2\right)\left[\cos \mathrm{h}\left(i\omega_n t\right) - \cos\left(\Omega_n t\right)\right] \end{array}\right\}. \tag{22}$$

Taking the Laplace transform for equation (19), while assuming homogenous conditions and considering that $J \geq 1$, yields to the following:

$$s^2 y_n^J(s) + \omega_n^2 y_n^J(s) = -2\omega_n\zeta_n s^\alpha y_n^{J-1}(s). \tag{23}$$

Rearranging equation (23), the recursive formula for the solution is obtained as follows:

$$y_n^J(s) = \frac{-2\omega_n\zeta_n s^\alpha}{\left(s^2+\omega_n^2\right)} y_n^{J-1}(s). \tag{24}$$

So, using equation (24) with the aid of the value $y_n^0(s)$ from equation (21) and applying math induction, the general form of $y_n^J(s)$ for $J \geq 1$ is written as follows:

$$y_n^J(s) = \frac{(-1)^J P_0\Phi_n(s)\left(2\omega_n\zeta_n s^\alpha\right)^J}{\chi_n\left(s^2+\omega_n^2\right)^{J+1}}. \tag{25}$$

Then, the total series solution, in the Laplace domain, is written as follows:

$$y_n(s) = \frac{P_0\Phi_n(s)}{\chi_n\left(s^2+\omega_n^2\right)} + \sum_{J=1}^{\infty} \frac{(-1)^J P_0\Phi_n(s)\left(2\omega_n\zeta_n s^\alpha\right)^J}{\chi_n\left(s^2+\omega_n^2\right)^{J+1}}. \tag{26}$$

This can be rearranged as follows:

$$y_n(s) = \frac{P_0\Phi_n(s)}{\chi_n\left(s^2+\omega_n^2\right)} + \frac{P_0\Phi_n(s)}{\chi_n\left(s^2+\omega_n^2\right)} \sum_{J=1}^{\infty}\left[\left(\frac{-2\omega_n\zeta_n s^\alpha}{s^2+\omega_n^2}\right)^J\right]. \tag{27}$$

Comparing the series in equation (27) with the general form of the geometric series, that is,

$$\sum_{J=a}^{b}\left(\Upsilon\,\mathfrak{R}^J\right) = \frac{\Upsilon\left(\mathfrak{R}^a - \mathfrak{R}^{b+1}\right)}{1-\mathfrak{R}}. \tag{28}$$

In this, $\Upsilon = P_0\Phi_n(s)/\chi_n(s^2+\omega_n^2)$ and $\mathfrak{R} = -2\omega_n\zeta_n s^\alpha/s^2+\omega_n^2$. Realizing that the quantities ω_n, ζ_n are positive values, then if $2\omega_n\zeta_n s^\alpha/s^2+\omega_n^2 < 1$, the summation presented in equation (27) according to equation (28) becomes the following:

$$y_n(s) = \frac{P_0\Phi_n(s)}{\chi_n\left(s^2+\omega_n^2\right)} + \frac{P_0\Phi_n(s)\left(-2\omega_n\zeta_n s^\alpha\right)}{\chi_n\left(s^2+\omega_n^2\right)\left(s^2+2\omega_n\zeta_n s^\alpha+\omega_n^2\right)}. \tag{29}$$

As a result, to find the solution in the time domain, it is desired to find the Laplace inverse for equation (29), and for this purpose, a number of cases will be studied hereafter.

2.1. Elastic Beam. Beams behave elastically when the damping ratio equals zero; therefore, the closed-form solution of the elastic beam can be written as follows:

$$Y_n(t) = \frac{P_0}{\omega_n \chi_n \left(\Omega_n^4 - \omega_n^4\right)} \begin{bmatrix} \left[\omega_n^2 + \Omega_n^2\right]\left[\Omega_n \sin\left(\omega_n t\right) - \omega_n \sin\left(\Omega_n t\right)\right] \\ + \omega_n A_n \left[\omega_n^2 + \Omega_n^2\right]\left[\cos\left(\omega_n t\right) - \cos\left(\Omega_n t\right)\right] \\ + B_n \left[\omega_n^2 - \Omega_n^2\right]\left[\Omega_n \sin\left(\omega_n t\right) - \omega_n \sin \mathrm{h}\left(\Omega_n t\right)\right] \\ + \omega_n C_n \left(\omega_n^2 - \Omega_n^2\right)\left(\cos\left(\omega_n t\right) - \cos \mathrm{h}\left(\Omega_n t\right)\right) \end{bmatrix}. \tag{30}$$

To verify the validity of this solution, the simply supported beam case is considered, and the coefficients of the vibration mode in equation (30) are all set to zero, then the solution becomes the following:

$$Y_n(t) = \frac{P_0}{\chi_n \left(\omega_n^2 - \Omega_n^2\right)} \left[\sin\left(\Omega_n t\right) - \frac{\Omega_n \sin\left(\omega_n t\right)}{\omega_n}\right]. \tag{31}$$

This equation represents exactly the same result obtained by other formulations made in the literature (Rao [30] and Abu-Malloh et al. [31]). Finally, by substituting equation (30), with equation (4), the transverse displacement of the system $w(x,t)$ at point x and time t for the elastic beam can be written in the following form:

$$w(x,t) = \sum_{n=1}^{N} \left\{ \frac{P_0 \varphi_n(x)}{\omega_n \chi_n \left(\Omega_n^4 - \omega_n^4\right)} \begin{bmatrix} \left(\omega_n^2 + \Omega_n^2\right)\left(\Omega_n \sin\left(\omega_n t\right) - \omega_n \sin\left(\Omega_n t\right)\right) \\ + \omega_n A_n \left(\omega_n^2 + \Omega_n^2\right)\left(\cos\left(\omega_n t\right) - \cos\left(\Omega_n t\right)\right) \\ + B_n \left(\omega_n^2 - \Omega_n^2\right)\left(\Omega_n \sin\left(\omega_n t\right) - \omega_n \sin \mathrm{h}\left(\Omega_n t\right)\right) \\ + \omega_n C_n \left(\omega_n^2 - \Omega_n^2\right)\left(\cos\left(\omega_n t\right) - \cos \mathrm{h}\left(\Omega_n t\right)\right) \end{bmatrix} \right\}. \tag{32}$$

2.2. Integer Order Damped Beam. Considering the viscous beam described by the Kelvin–Voigt model while being affected by a moving load with constant velocity, then the generalized displacement of this special case can be obtained as

$$Y_n(t) = Y_{n1}(t) + Y_{n2}(t) + Y_{n3}(t) + Y_{n4}(t), \tag{33}$$

where

$$Y_{n1}(t) = \frac{P_0}{\chi_n Z_2} \left\{ \begin{array}{c} \frac{1}{Z_1}\left[\Omega_n \left(2\omega_n^2 \zeta_n^2 + \Omega_n^2 - \omega_n^2\right) \sin \mathrm{h}\left(Z_1 t\right)\left[\cos \mathrm{h}\left(\omega_n \zeta_n t\right) - \sin \mathrm{h}\left(\omega_n \zeta_n t\right)\right]\right] \\ + 2\omega_n \zeta_n \Omega_n \left[\cos \mathrm{h}\left(Z_1 t\right)\left[\cos \mathrm{h}\left(\omega_n \zeta_n t\right) - \sin \mathrm{h}\left(\omega_n \zeta_n t\right)\right] - \cos\left(\Omega_n t\right)\right] - Z_3 \sin\left(\Omega_n t\right) \end{array} \right\},$$

$$Y_{n2}(t) = \frac{P_0 A_n}{\chi_n Z_2} \left\{ \begin{array}{c} \frac{1}{Z_1}\left[\omega_n \zeta_n Z_4 \sin \mathrm{h}\left(Z_1 t\right)\left(\sin \mathrm{h}\left(\omega_n \zeta_n t\right) - \cos \mathrm{h}\left(\omega_n \zeta_n t\right)\right)\right] + 2\Omega_n \omega_n \zeta_n \sin\left(\Omega_n t\right) \\ + Z_3 \left[\cos \mathrm{h}\left(Z_1 t\right)\left(\cos \mathrm{h}\left(\omega_n \zeta_n t\right) - \sin \mathrm{h}\left(\omega_n \zeta_n t\right)\right) - \cos\left(\Omega_n t\right)\right] \end{array} \right\},$$

$$Y_{n3}(t) = \frac{P_0 B_n}{2\chi_n Z_2} \left\{ \begin{array}{c} \frac{1}{Z_1 Z_5}\left[2\Omega_n \left(-2\omega_n^2 \zeta_n^2 + \Omega_n^2 + \omega_n^2\right) \sin \mathrm{h}\left(Z_1 t\right)\left[\cos \mathrm{h}\left(\omega_n \zeta_n t\right) - \sin \mathrm{h}\left(\omega_n \zeta_n t\right)\right]\right] \\ -\frac{1}{Z_5}\left[\begin{array}{c} 4\Omega_n \omega_n \zeta_n \left[\cos \mathrm{h}\left(Z_1 t\right)\left[\cos \mathrm{h}\left(\omega_n \zeta_n t\right) - \sin \mathrm{h}\left(\omega_n \zeta_n t\right)\right] - 2\cos \mathrm{h}\left(\Omega_n t\right)\right] \\ 2\sin \mathrm{h}\left(\Omega_n t\right)\left[\Omega_n^2 + \omega_n^2\right] \end{array}\right] \end{array} \right\}, \tag{34}$$

$$Y_{n4}(t) = \frac{P_0 C_n}{2\chi_n Z_5} \left\{ \begin{array}{c} \frac{1}{Z_1}\left[2\omega_n \zeta_n Z_3 \sin \mathrm{h}\left(Z_1 t\right)\left[\sin \mathrm{h}\left(\omega_n \zeta_n t\right) - \cos \mathrm{h}\left(\omega_n \zeta_n t\right)\right]\right] \\ -\left(2\Omega_n \omega_n \zeta_n + \Omega_n^2 + \omega_n^2\right)\left(\cos \mathrm{h}\left(\Omega_n t\right) - \sin \mathrm{h}\left(\Omega_n t\right)\right) \\ -2Z_4 \cos \mathrm{h}\left(Z_1 t\right)\left[\sin \mathrm{h}\left(\omega_n \zeta_n t\right) - \cos \mathrm{h}\left(\omega_n \zeta_n t\right)\right] \\ +\left(-2\Omega_n \omega_n \zeta_n + \Omega_n^2 + \omega_n^2\right)\left(\cos \mathrm{h}\left(\Omega_n t\right) + \sin \mathrm{h}\left(\Omega_n t\right)\right) \end{array} \right\},$$

in which

$$\begin{aligned} Z_1 &= \omega_n\sqrt{\zeta_n^2 - 1}, \\ Z_2 &= 4\Omega_n^2\omega_n^2\zeta_n^2 + Z_3^2, \\ Z_3 &= \Omega_n^2 - \omega_n^2, \\ Z_4 &= \Omega_n^2 + \omega_n^2, \\ Z_5 &= 4\Omega_n^2\omega_n^2\zeta_n^2 - Z_4^2. \end{aligned} \tag{35}$$

Finally, by substituting equation (33) in equation (4), then $w(x,t)$ for the beam with integer order damping can be written in the following form:

$$w(x,t) = \sum_{n=1}^{N} Y_n(t)\left[\sin(\gamma_n x) + A_n\cos(\gamma_n x) + B_n\sin\mathrm{h}(\gamma_n x) + C_n\cos\mathrm{h}(\gamma_n x)\right]. \tag{36}$$

2.3. Fractional Kelvin–Voigt Model. In this section, the fractional Kelvin–Voigt modeled beam is studied; the beam is assumed to be fractional with order of α, where $0 \le \alpha \le 1$, referring to equation (29), and the recursive formula for this beam in the Laplace domain can be written as follows:

$$y_n(s) = \frac{P_0\Phi_n(s)}{\chi_n\left(s^2 + \omega_n^2\right)} - \frac{2P_0\Phi_n(s)\omega_n\zeta_n s^{\alpha}}{\chi_n\left(s^2 + \omega_n^2\right)\left(s^2 + 2\omega_n\zeta_n s^{\alpha} + \omega_n^2\right)} = y_{n0}(s) - y_{n1}(s). \tag{37}$$

For the first term, $y_{n0}(s)$, the direct Laplace inverse is used to find the solution, as it was previously achieved in equation (22). Then, Laplace inversion for $y_{n1}(s)$ term can be obtained by applying the convolution theorem as follows:

$$y_{n1}(s) = \frac{2\omega_n\zeta_n P_0 s^{\alpha}\Phi_n(s)}{\chi_n\left(s^2 + \omega_n^2\right)\left(s^2 + 2\omega_n\zeta_n s^{\alpha} + \omega_n^2\right)} = \left[\frac{2\omega_n\zeta_n P_0\Phi_n(s)}{\chi_n\left(s^2 + \omega_n^2\right)}\right]\left(\frac{s^{\alpha}}{s^2 + 2\omega_n\zeta_n s^{\alpha} + \omega_n^2}\right) = f(s)\,g(s). \tag{38}$$

For $f(s)$, Laplace inverse is directly obtained as follows:

$$F(t) = \frac{2\zeta_n P_0}{\chi_n\left(\Omega_n^4 - \omega_n^4\right)}\begin{bmatrix} \left(\Omega_n^2 + \omega_n^2\right)\left(\Omega_n\sin\omega_n t - \omega_n\sin\Omega_n t\right) \\ + A_n\omega_n\left(\Omega_n^2 + \omega_n^2\right)\left(\cos\omega_n t - \cos\Omega_n t\right) \\ - B_n\left(\Omega_n^2 - \omega_n^2\right)\left(\Omega_n\sin\omega_n t - \omega_n\sin\mathrm{h}\Omega_n t\right) \\ - C_n\omega_n\left(\Omega_n^2 - \omega_n^2\right)\left(\cos\omega_n t - \cos\mathrm{h}\Omega_n t\right) \end{bmatrix}. \tag{39}$$

For $g(s)$, the following fractional Green's function of the third order is used to obtain the Laplace inverse (Podlubny [8]) as follows:

$$G(t) = \frac{1}{a}\sum_{k=0}^{\infty}\left[\frac{(-1)^k}{k!}\left(\frac{c}{a}\right)^k t^{\xi(k+1)-1}E^{(k)}_{\xi-\psi,\xi+\psi k}\left(-\frac{b}{a}t^{\xi-\psi}\right)\right]. \tag{40}$$

Then, $g(s)$ can be rewritten as follows:

$$g(s) = \frac{1}{s^{2-\alpha} + \omega_n^2 s^{-\alpha} + 2\omega_n\zeta_n}. \tag{41}$$

The coefficients are as follows:

$$a = 1, b = \omega_n^2, c = 2\omega_n\zeta_n, \xi = 2 - \alpha, \psi = -\alpha. \tag{42}$$

Hence, $G(t)$ becomes

$$G(t) = \sum_{k=0}^{\infty} \frac{(-1)^k}{k!} (2\omega_n \zeta_n)^k t^{(2-\alpha)(k+1)-1} E_{2,2-\alpha+\alpha k}^{(k)}\left(-\omega_n^2 t^2\right), \tag{43}$$

where $E_{2,2-\alpha+\alpha k}^{(k)}(-\omega_n^2 t^2)$ is the k^{th} derivative of the Mittag–Leffler function, which is defined as follows:

$$E_{2,2-\alpha+\alpha k}^{(k)}\left(-\omega_n^2 t^2\right) = \sum_{j=0}^{\infty} \frac{(j+k)!\left(-\omega_n^2 t^2\right)^j}{j!\,\Gamma(2j+2k+\beta-\alpha k)}. \tag{44}$$

So, equation (40) becomes the following:

$$G(t) = \sum_{k=0}^{\infty} \frac{(-1)^k}{k!} (2\omega_n \zeta_n)^k \left(t^{(2-\alpha)(k+1)-1}\right) \cdot \sum_{j=0}^{\infty} \frac{(j+k)!\left(-\omega_n^2 t^2\right)^j}{j!\,\Gamma(2j+2k+\beta-\alpha k)}. \tag{45}$$

Now, applying the convolution theorem for the functions presented in equations (39) and (45) leads to

$$Y_{n1}(t) = F(t) * G(t) = \int_0^t F(t-\tau)\, G(\tau)\, \mathrm{d}\tau. \tag{46}$$

The solution of the integration in equation (46) is found analytically by rearranging equation (45) as follows:

$$G(t) = \sum_{k=0}^{\infty} \sum_{j=0}^{\infty} \frac{(-1)^k (2\omega_n \zeta_n)^k (j+k)!\left(-\omega_n^2\right)^j}{k!\, j!\, \Gamma(2j+2k+\beta-\alpha k)} \cdot t^{(2-\alpha)(k+1)+2j-1}. \tag{47}$$

Defining the following parameters, we have

$$H = H(k,j) = (2-\alpha)(k+1) + 2j, \tag{48}$$

$$\vartheta_1 = \vartheta_1(k,j) = \frac{(-1)^k (2\omega_n \zeta_n)^k (j+k)!\left(-\omega_n^2\right)^j}{k!\, j!\, \Gamma(2j+2k+\beta-\alpha k)}. \tag{49}$$

Hence, $G(t)$ becomes the following:

$$G(t) = \sum_{k=0}^{m} \left[\sum_{j=0}^{\infty} \vartheta_1\, t^{H-1}\right]. \tag{50}$$

By computing integration in equation (46) term by term, the value of $Y_{n1}(t)$ is found as a summation of the following four equations:

$$\begin{aligned}
Y_{n1a}(t) &= \frac{2P_0 \zeta_n \omega_n \Omega_n t^{H+1}}{\chi_n\left(\Omega_n^2 - \omega_n^2\right) H(H+1)} \left\{ \frac{\mathrm{LommelS1}\left(3/2H, 1/2\omega_n t\right)}{\left(\omega_n t\right)^{H+1/2}} - \frac{\mathrm{LommelS1}\left(3/2H, 1/2\Omega_n t\right)}{\left(\Omega_n t\right)^{H+1/2}} \right\}, \\
Y_{n1b}(t) &= \frac{2P_0 A_n \zeta_n \omega_n t^{H+1}}{\chi_n\left(\Omega_n^2 - \omega_n^2\right) H(H+1)} \left\{ \begin{array}{l} \dfrac{H\,\mathrm{LommelS1}\left(1/2H, 3/2\omega_n t\right)}{\left(\omega_n t\right)^{H+1/2}} - \dfrac{\Omega_n H\,\mathrm{LommelS1}\left(1/2H, 3/2\Omega_n t\right)}{\left(\Omega_n t\right)^{H+1/2}} \\ + \dfrac{\mathrm{LommelS1}\left(3/2H, 1/2\omega_n t\right)}{t\left(\omega_n t\right)^{H+1/2}} - \dfrac{\mathrm{LommelS1}\left(3/2H, 1/2\Omega_n t\right)}{t\left(\Omega_n t\right)^{H+1/2}} \end{array} \right\}, \\
Y_{n1c}(t) &= \frac{2P_0 \zeta_n \omega_n B_n \Omega_n t^{H+1}}{\chi_n\left(\Omega_n^2 + \omega_n^2\right) H(H+1)} \left\{ \frac{\mathrm{LommelS1}\left(3/2H, 1/2\omega_n t\right)}{\left(\omega_n t\right)^{H+1/2}} - \frac{\mathrm{hypergeom}\left([1], [1+1/2, 3/2+1/2H], 1/4\Omega_n^2 t^2\right)}{\left(\Omega_n t\right)^{H+1/2}} \right\}, \\
Y_{n1d}(t) &= \frac{2P_0 C_n \zeta_n \omega_n}{\chi_n\left(\Omega_n^2 - \omega_n^2\right) H(H+1)} \left\{ \begin{array}{l} \dfrac{H\omega_n t^{H+1}\,\mathrm{LommelS1}\left(1/2H, 3/2\omega_n t\right)}{\left(\omega_n t\right)^{H+1/2}} - \dfrac{t^H\,\mathrm{LommelS1}\left(3/2H, 1/2\omega_n t\right)}{\left(\omega_n t\right)^{H+1/2}} \\ + \dfrac{\mathrm{LommelS1}\left(3/2H, 1/2\omega_n t\right)}{t\left(\omega_n t\right)^{H+1/2}} - \dfrac{\mathrm{LommelS1}\left(3/2H, 1/2\Omega_n t\right)}{t\left(\Omega_n t\right)^{H+1/2}} \end{array} \right\}.
\end{aligned} \tag{51}$$

Thus,

$$Y_{n1}(t) = \sum_{k=0}^{\infty} \left[\sum_{j=0}^{\infty} \vartheta_1 \left[Y_{n1a}(t) + Y_{n1b}(t) + Y_{n1c}(t) + Y_{n1d}(t)\right]\right], \tag{52}$$

where the *hypogeom*(.) and *LommelS1*(.) are the generalized hypergeometric and generalized Lommel special functions, respectively, and then $Y_n(t)$ is obtained by adding the two solutions in equations (22) and (52). Finally, $w(x,t)$ for the fractionally damped beam can be written in the following form:

$$w(x,t) = \sum_{n=1}^{N} Y_n(t) \left[\sin\left(\gamma_n x\right) + A_n \cos\left(\gamma_n x\right) + B_n \sin \mathrm{h}\left(\gamma_n x\right) + C_n \cos \mathrm{h}\left(\gamma_n x\right)\right]. \tag{53}$$

All the solutions of the previously presented formulations are truncated and fulfilled using the mathematical software package, Maple.

3. Results and Discussion

In this section, a numerical verification will initially be presented to verify the obtained formulation in the previous section, and then the application of these equations is extended to plot the generalized deflection response of the beam to a moving load for the four BCs considered. Moreover, the proposed results are to be compared to those corresponding results present in the literature obtained using different approaches. Finally, the effects of the load normalized velocity, damping ratio, and the order of the fractional derivative on the beam's response are presented and discussed.

3.1. Numerical Verification of the Formulations. In order to perform the numerical verification of the solutions of equations for the first mode shape ($n = 1$) and after considering that the nondimensional length of the beam is unity, some arbitrary set of parameters are taken as follows:

$$\begin{aligned} &P_0 = 254.365465\,N \quad \mu = 3000\,\frac{\text{kg}}{m} \quad L = 1\,m \quad \text{EI} = 215280\,\text{Nm}, \\ &\omega_1 = 4.654654\,\frac{\text{rad}}{s} \quad \Omega_1 = 25.654645\,\frac{\text{rad}}{s} \quad \gamma_1 = 1.6541654m^{-1} \quad \chi_1 = 1565.654, \\ &t = 0.06546\,s \quad A_1 = 0.3512613 \quad B_1 = 0.19414165 \quad C_1 = 0.89747. \end{aligned} \tag{54}$$

These parameters are to be substituted in the corresponding equations to obtain the response of the beam in terms of maximum deflection. It is important to mention that, for most results shown in this section, a nondimensional analysis is practiced, for which the units of the above parameters are eliminated, and this practice is advantageous to generalize the results for any desired set of data.

Firstly, the response of the elastic beam case in terms of maximum deflection at midpoint of the PP beam due to the moving load is calculated by the closed-form solution, as shown in equation (30). The resulted values of this solution are considered as control. Then, the beam with integer order damping case equations are used to calculate the response of the elastic beam, which can be achieved by setting the value of ζ to be approaching zero. Systematically, the elastic beam response is recalculated by the fractional Kelvin–Voigt beam equations. In this case, both $\alpha$and ζ are set to be approaching zero. Both results from integer order damped and fractional order Voigt equations are compared to the control solution as listed for each term in Table 2.

It can be seen from Table 2 that, for the simple case of elastic beam, all equations obtained within this contribution provided almost the same solutions with an error approaching zero percent. It is worth noting that results from the first mode of vibration are used in the whole paper because it is proved to be the most effective one in such beam cases.

The same procedure of verification is performed this time by solving integer order damped PP beam case using equation (33) by setting $\zeta = 0.25$ and then comparing the resulted deflection at beam midspan to those obtained using the fractional Voigt beam equations when $\alpha = 1$ and $\zeta = 0.25$, which in this case represents a beam with integer order damping.

Table 3 shows that the solution of deflection obtained from the integer order damping solution fits exactly into the solution obtained from the fractional beam equations, which implies that both elastic and integer order damping beam cases can be solved by the proposed set of fractional beam equations.

3.2. Effect of the Moving Load Velocity. In order to generalize the representation of the solution of the beam, dimensionless parameters are introduced, namely, dimensionless speed (β) of the moving load, which is the ratio of the load speed (v) to the load critical speed (C_{cr}), and the dimensionless time ($\overline{t}$), which equals to tv/L. Here, $C_{cr} = \omega_1 L/\pi$ as mentioned in the study by Hilal and Zibdeh [4]. The normalized beam deflection then can be defined as follows:

$$\overline{w}(x_{\max}, \overline{t}) = \frac{w(x_{\max}, \overline{t})}{(\text{STD})_{\max}}, \tag{55}$$

where $x_{\max}$ and $(\text{STD})_{\max}$ are location and value of the maximum static deflection of the beam, respectively, and the normalized position $\overline{x}$ is defined as the position along the beam (x) divided by the beam length (L), as $\overline{x} = x/L$.

In Figure 1, the normalized elastic beam deflections versus the dimensionless time are plotted for PP, FF, FF, and FC beams, considering five different load velocities: $\beta = 0.05, 0.2, 0.5, 0.8$, and 1. The curves of these figures conform well with those obtained in the literature considering similar parameters (Foda and Abduljabbar [33] and Fryba [34]). Moreover, from Figure 1, it can be clearly seen that at lower velocity, the response reaches its peak at a certain value of $\overline{t}$ and then decreases to zero at $\overline{t} = 1$. While at higher velocities, the peak is shifted to the right, and it is still high at $\overline{t} = 1$. Moreover, the response of the beam increases by increasing the velocity, until it reaches its peak at $\beta = 0.5$, and then the maximum response values start to decrease as β increases. On the other hand, at very low velocities, the response behavior is reciprocating since the moving load is not able to deform the beam effectively, while at higher velocities, the response behavior is more obviously affected by the moving load. In order to compare the response of the four types of beams under the moving load, $\beta = 0.5$ is chosen

Table 2: Deflection of elastic beam.

Eqn. term	By elastic case equations (control)	By integer order damping case equations		By fractional order damping case equations	
	Deflection	Deflection	Error (%)	Deflection	Error (%)
1st	0.0001685609707709	0.0001685609707709	0	0.0001685609707709	0
2nd	0.0000953743185763	0.0000953743185763	0	0.0000953743185763	0
3rd	0.0000434171060674	0.0000434171060674	0	0.0000434171060674	0
4th	0.0003910063958128	0.0003910063958128	0	0.0003910063958128	0

Table 3: Deflection of beam with integer order damping.

Eqn. term	By integer order damping case equations	By fractional order damping case equations	
	Deflection	Deflection	Error (%)
1st	0.00016205306007776	0.00016205306005099	1.65×10^{-8}
2nd	0.00090246447172046	0.00090246447172822	8.60×10^{-10}
3rd	0.00041888988041822	0.00041888988041144	1.62×10^{-9}
4th	0.00037354980321408	0.00037354980321542	3.58×10^{-10}

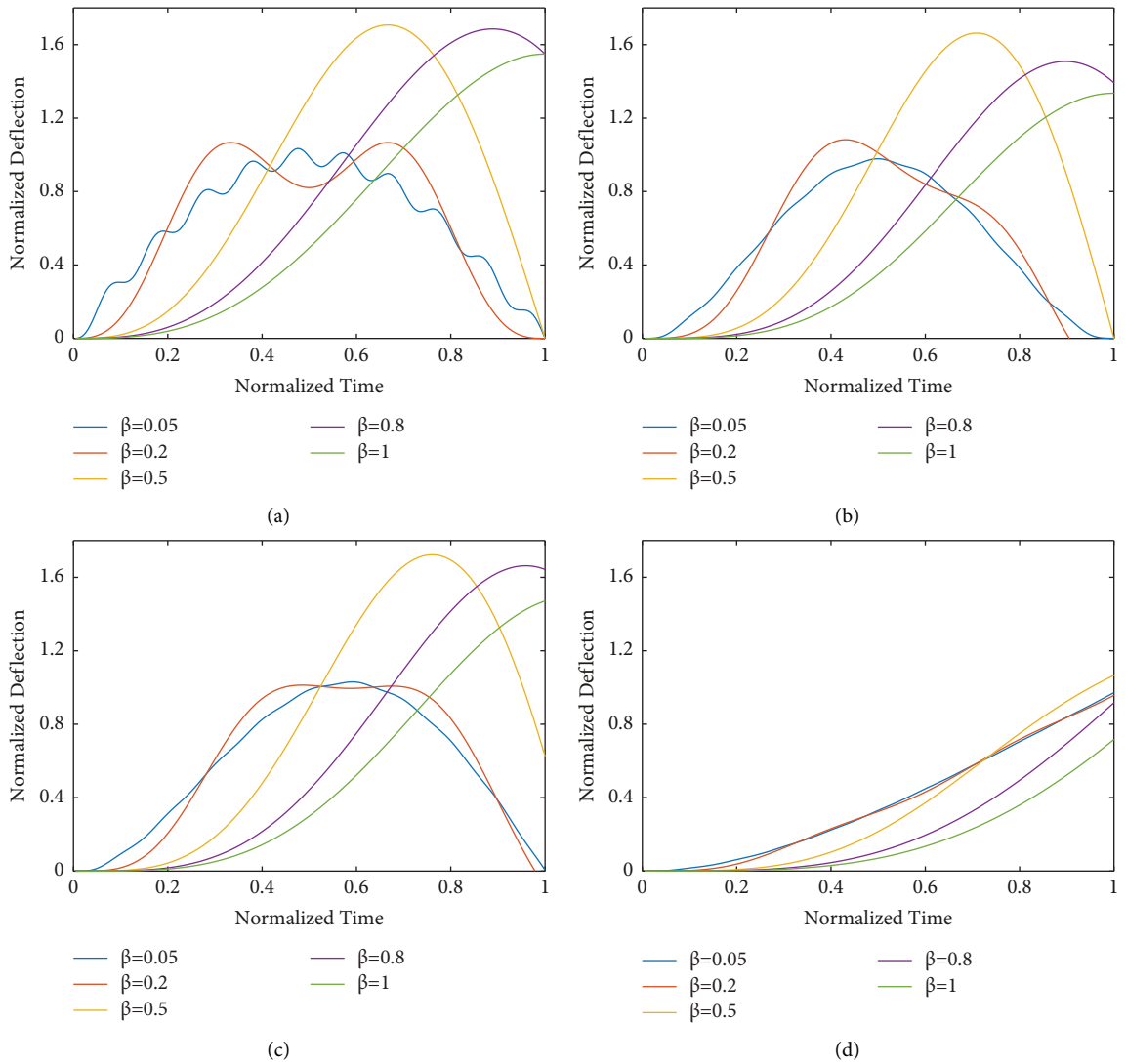

Figure 1: Maximum response of elastic beam at different β values. (a) Pinned-pinned, (b) fixed-fixed, (c) fixed-pinned, and (d) fixed-free.

Table 4: Maximum deflection of elastic beams with the normalized time.

Beam end conditions	Position of max. deflection (m)	Time corresponds to max. deflection (sec)	Max. normalized deflection
PP	0.5	0.665	1.70694872328
FF	0.5	0.71	1.66289273724
FP	0.554	0.7605	1.72303418723
FC	1.0	1.0	1.06559158286

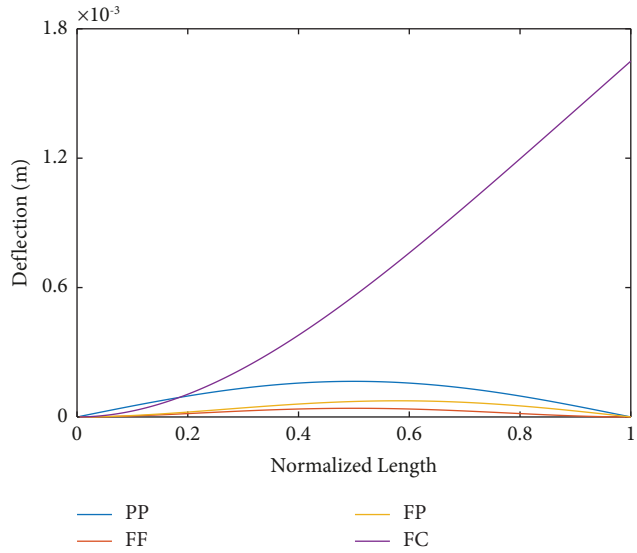

Figure 2: Maximum dimensional response of the four boundary conditions of elastic beams at $\beta = 0.5$ with the normalized length.

as a speed parameter since the response at this velocity is relatively high compared with other velocities. Table 4 lists the maximum normalized deflection of the four types of beams at $\beta = 0.5$, as shown in Figures 1 and 2, which show a comparison for the actual (dimensional) beams' response along the normalized beam length. From Table 4 and Figure 2, the maximum beam deflection occurs earlier, in terms of time and distance, in the PP beam than the other cases.

3.3. Effect of Damping Ratio. In general, when increasing the damping ratio, the response of the beam is normally decreased; to check if this applies on the results of the proposed formulations and to compare with the previously obtained results by other approaches, Figure 3 is plotted to show the response of the beam with integer order damping under varying damping ratios ($\zeta = 0$, 0.1, 0.2, and 0.3). The curves of these figures fit exactly into the results obtained in the literature by Hilal and Zibdeh [4]. The effect of the damping ratio is clear in this figure; as for $\zeta = 0.0$, the beam demonstrated exact elastic response, and when increasing ζ, responses get closer to each other, while at $\overline{t} = 1$, all the responses are almost zero.

Figure 4 shows the dynamic response of the four beams when $\beta = 0.5$ and $\zeta = 0, 0.1, 0.2,$ and 0.3. The curves of this figure confirm that when $\zeta = 0$, beams respond elastically; however, when increasing the damping ratio, the peak deflection decreases and gets shifted to a higher value of $\overline{t}$. Also, the deflection of the beam in the figures decreased when the damping ratio increased, and this result agrees with the concept of damping since the damping reduces the vibration effect of the beam.

Table 5 lists the percentage reduction of the peak normalized deflection for each type of beam under study, in which the PP case exhibited more reduction percent in its normalized deflection than the other cases.

An attempt to study the effect of the moving load velocity on the beam response at different damping ratios is made by plotting Figure 5. This figure, in particular Figure 5(a), exhibits that the same trend appeared in similar figures found in the literature [4], while Figure 6 compares the response of different end condition beams when they are damped with integer order at $\beta = 0.5$ and $\zeta = 0.1$.

3.4. Effect of the Fractional Derivative. In this subsection, the effect of the beam's fractional derivative order to the beam's response is investigated, and this effect is not widely studied in the literature, especially for general beam BCs. Nevertheless, for the simply supported beams' case, some previous works [35] are found and compared to the results of the present work. Figures 7 and 8 are plotted to demonstrate the effect of a wide range of varied velocities of moving load on the midspan responses of the PP and FF beam, respectively, when fractional order $\alpha = 0.5$, while in Figure 9, the fractional derivative α is varying and the responses of the beam to a moving load of $\beta = 0.5$ are plotted. The damping ratio for all of these figures is taken as $\zeta = 0.1$. When comparing the curves of Figure 7 to the curves of the available cases in the

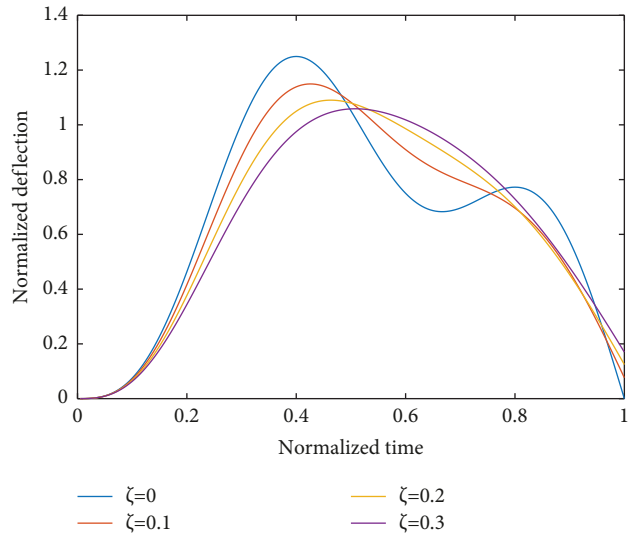

Figure 3: Dynamic response for pinned-pinned beam with integer order damping at $\beta = 0.25$.

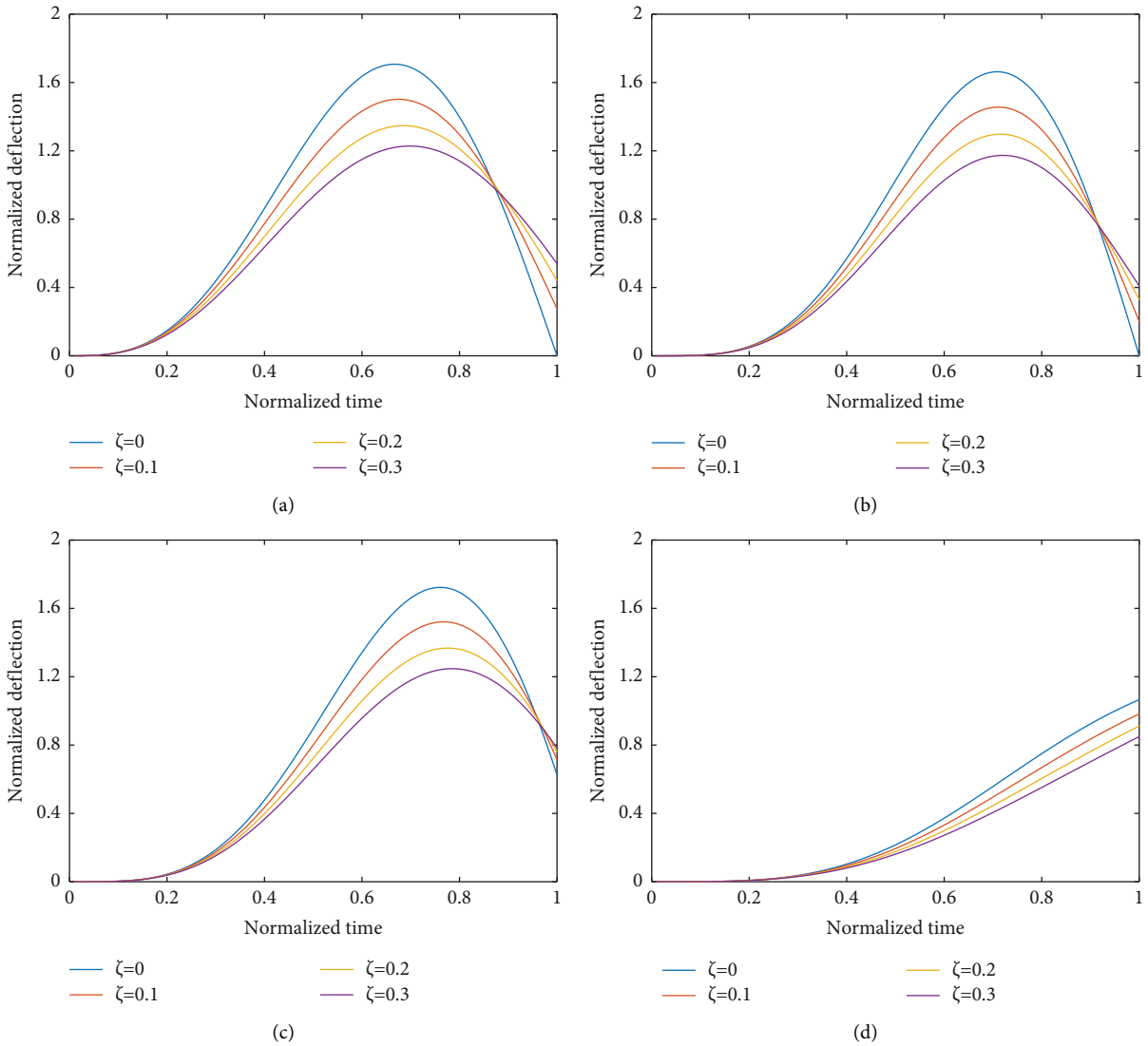

Figure 4: Maximum normalized response of beams with integer order damping at $\beta = 0.5$. (a) Pinned-pinned, (b) fixed-fixed, (c) fixed-pinned, and (d) fixed-free.

Table 5: Comparison of the maximum deflection of elastic beams and damped beams with integer order at $\beta = 0.5$.

Beam BC	Maximum dynamic deflection		
	Elastic beam	Damped beam with integer order	Percentage reduction (%)
PP	1.70694872328	1.500448614128	12.1
FF	1.66289273724	1.455719563051	12.5
FP	1.72303418723	1.521338905741	11.7
FC	1.06559158286	0.9824228067444	7.8

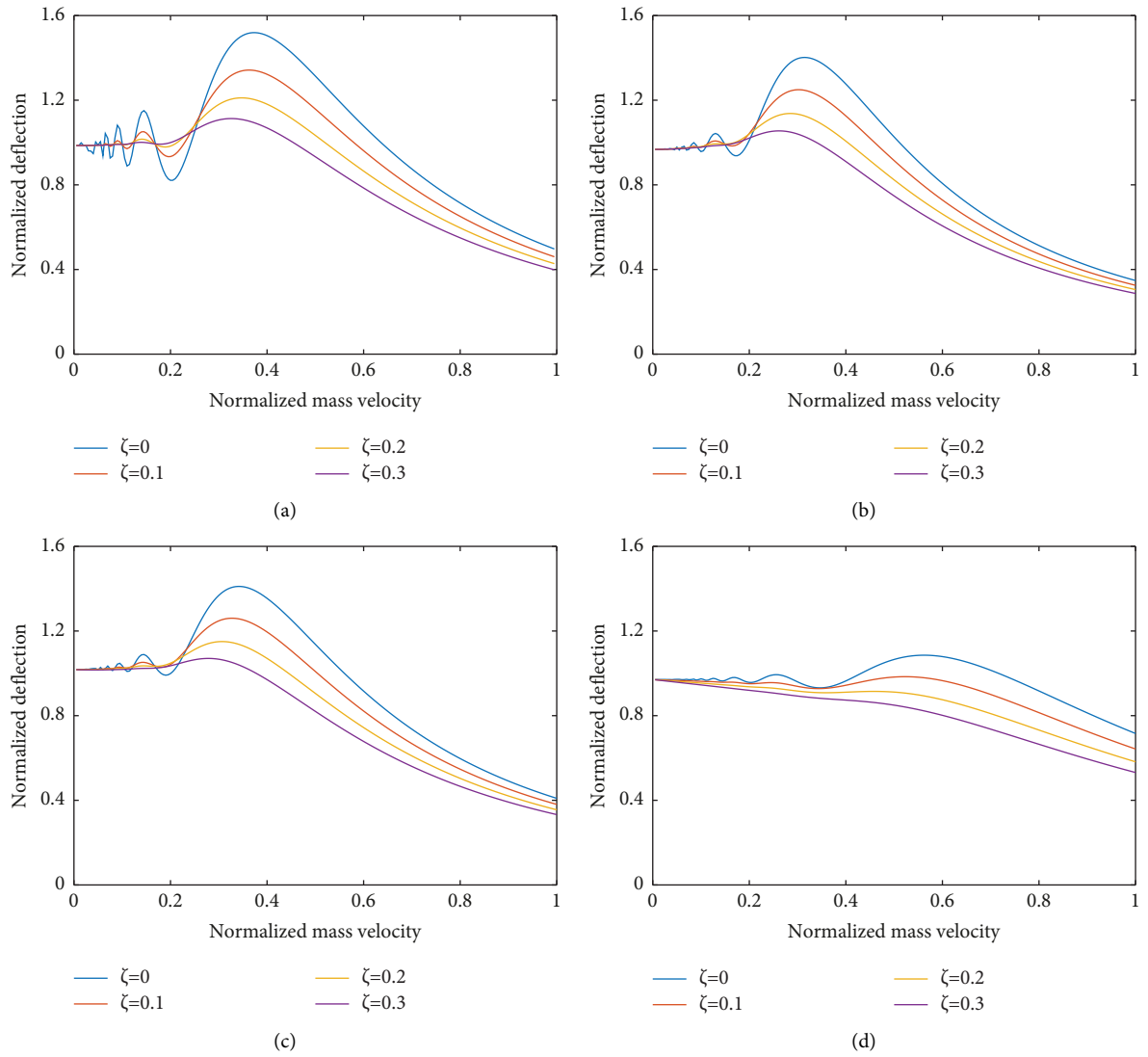

Figure 5: Variations of the normalized deflection with the velocity of the moving load. (a) Pinned-pinned, (b) fixed-fixed, (c) fixed-pinned, and (d) fixed-free.

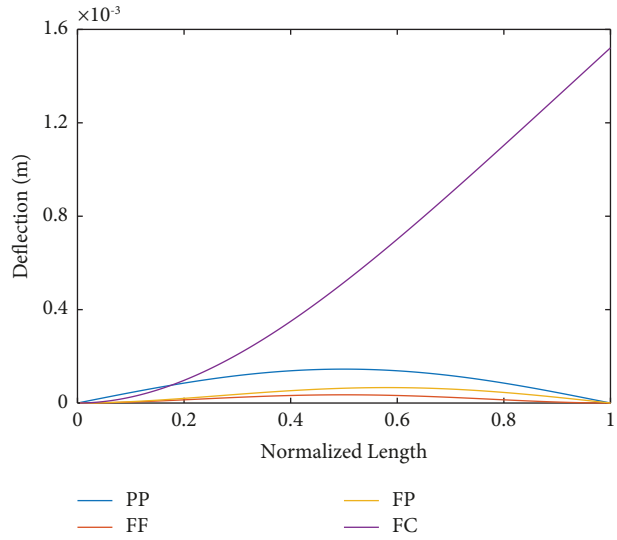

Figure 6: Maximum dimensional response of damped beams with integer order of different boundary conditions at $\beta = 0.5$ and $\zeta = 0.1$.

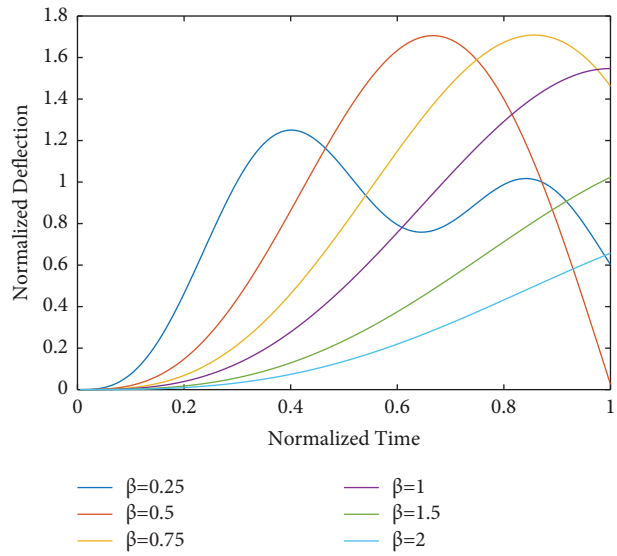

Figure 7: Dynamic response of the pinned-pinned beam at $\alpha = 0.5$ and varying β.

literature ($\beta = 0.25$, 0.5, 0.75, and 1 only), it can be said that this figure presents a solution that conforms to others presented previously (Freundlich [35]), while the curves of Figure 9 showed equal peaks' response to similar curves in the literature; however, differences appeared due to the numerical solution accuracy and to the effect of the damping ratio considered. Figure 9 implies that, by decreasing the order of the derivative, the response of the beam increases; nevertheless, the peak of the curve is not shifted, so the beam still reaches its peak value at the same time. Moreover, the noticeable effects of the fractional derivative on these curves are around the normalized peaks' region and at the end of the normalized time region rather than the rest of the curve regions. If the curves of Figures 7 and 8 are compared with the beams damped with the integer order, clear differences in the peak values are noticed; hence, decreasing the order of the fractional derivative yields to increasing the normalized deflection of the beams. In Figure 10, a comparison among the responses of fractionally damped beams of the four end conditions is presented at $\beta = 0.5$, $\zeta = 0.1$, and $\alpha = 0.5$. Table 6 supported by Figure 11 presents the maximum dimensional deflection of the elastic, integer order damped, and fractionally damped beams at different BCs, while $\zeta = 0.1$ and $\beta = 0.5$. The data in Table 6 show that for beam types studied, when increasing the order of the fractional derivative, deflection decreases; moreover, the response of the fractionally damped beams is always lower than the elastic beam and greater than the damped beam with integer order; that is, the behavior of the fractionally damped beam is intermediate between the elastic and fully viscous beam.

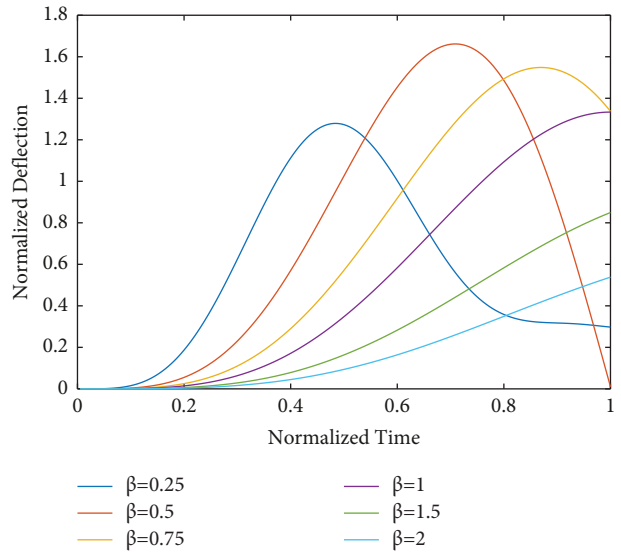

Figure 8: Dynamic response of the fixed-fixed beam at $\alpha = 0.5$ and varying β.

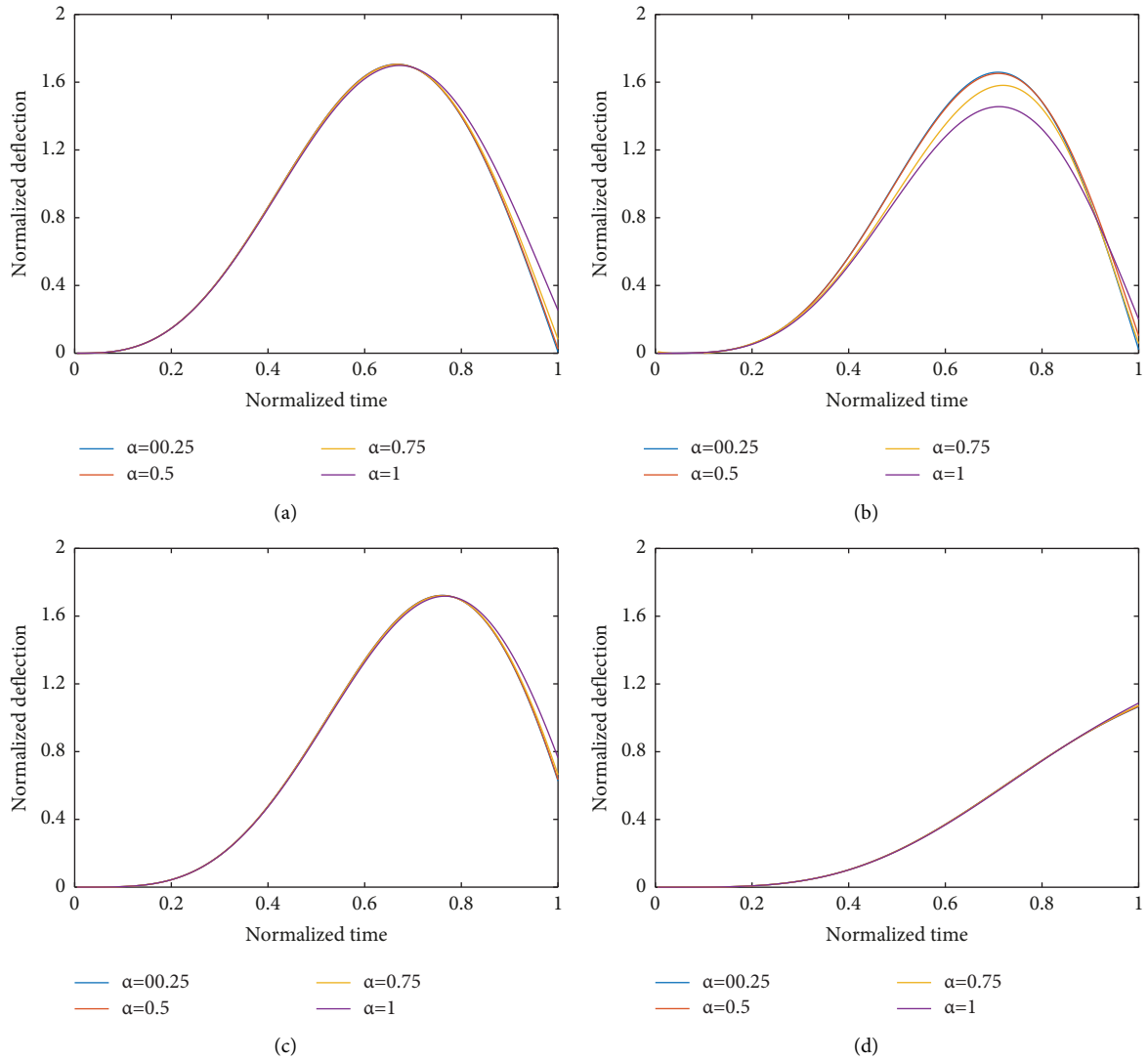

Figure 9: Dynamic deflections at the midspan of beam at various values of α when $\beta = 0.5$, (a) pinned-pinned, (b) fixed-fixed, (c) fixed-pinned, and (d) fixed-free.

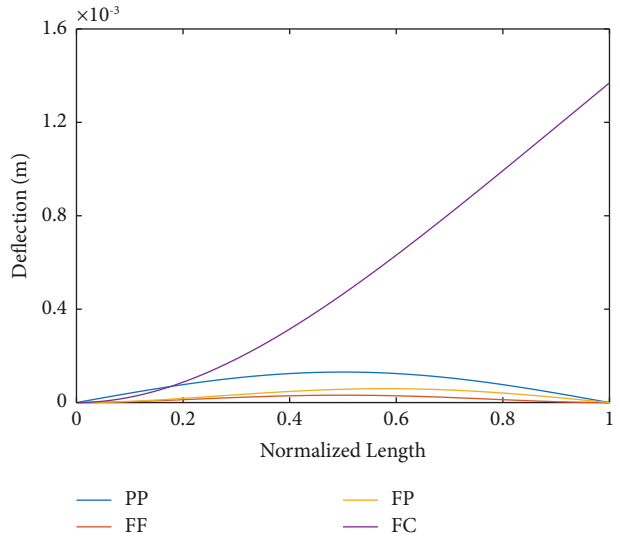

Figure 10: Maximum dimensional response of fractionally damped beams of different end conditions at $\beta = 0.5$, $\zeta = 0.1$, and $\alpha = 0.5$.

Table 6: Comparison of the maximum deflection of elastic, integer order damped, and fractionally damped beams when $\zeta = 0.1$ and $\beta = 0.5$.

Beam BCs	Maximum dynamic deflection of different types of beams				
	Elastic	Fractional $\alpha = 0.25$	Fractional $\alpha = 0.5$	Fractional $\alpha = 0.75$	Integer order damped
PP	1.706948723	1.694170748	1.671691038	1.616274628	1.500448614
FF	1.662892737	1.656430881	1.640546497	1.590357290	1.455719563
FP	1.723034187	1.671252915	1.654289293	1.611554490	1.521338905
FC	1.065591582	1.049447374	1.035502397	1.013632963	0.982422807

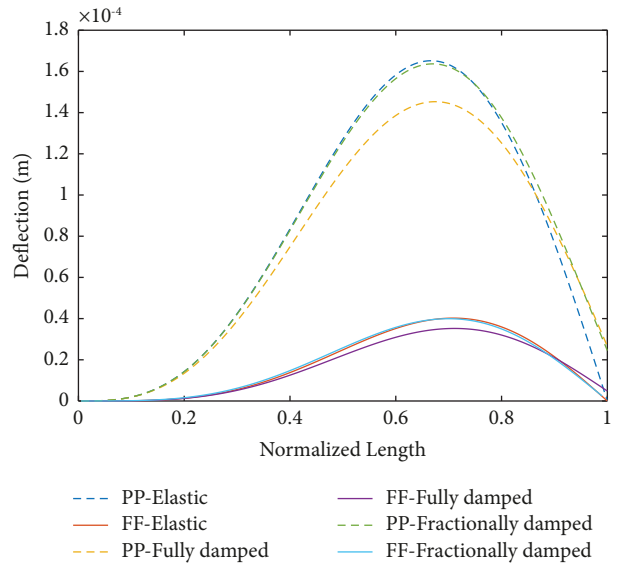

Figure 11: Maximum dimensional response of elastic, integer order damped, and fractional ($\alpha = 0.5$) pinned-pinned and fixed-fixed beams at $\beta = 0.5$.

4. Conclusions and Recommendations

This study investigated the dynamic response of Euler–Bernoulli beams of four different BCs with fractional order internal damping traversed by a moving load. An approach is introduced to obtain the closed-form solution of the problem based on Green's functions combined with the decomposition technique. Comparisons with the previous studies available in the literature for verification purposes showed great matching, and based on these verifications, further results were performed for cases that have not been available in the literature yet. The moving load effects were

investigated for a range of different values of constant velocity. In addition, the effects of the beams' dynamic response caused by the order of fractional derivative internal damping were also explored.

The main conclusion of this research is that the effects of using the fractional order derivative model containing fractional constitutive law gives some good consequences, despite the difficulties of using the fractional model due to the complicated math techniques and programming efforts.

From the obtained results and figures, the following conclusions can be also drawn:

(a) The amplitude of normalized deflection increases with the moving load velocity increase to a certain value, and then it starts to decrease.

(b) The beam dynamic oscillations were more evident for lower values of moving load velocities. In particular, PP beam suffered clearer oscillations.

(c) Positions of the beam's amplitude response shifts to the right when the load velocity increases.

(d) Among the investigated load velocities, the maximum beam normalized response appeared at $\beta = 0.5$ for all BCs.

(e) When damping ratio was decreased, beams suffered more oscillations and response amplitudes were shifted to the left.

(f) The largest amplitude of normalized deflection appeared for PP case and the lowest appeared for FC, while the largest amplitude of dimensional response appeared in the FC case and the lowest was for FF.

(g) The fractional order affected most of the amplitude response of FF and the least that of FC, while for PP and PF, effects were clearer at the time end.

(h) Beam deflection at $\alpha = 0.5$ is found to be less than the average deflection of those when $\alpha = 0.0$ (undamped case) and $\alpha = 1.0$ (one integer damping case), which implies that the deflection does not change linearly with the order of the fractional derivative α.

For any certain engineering application, further future research can be implemented, in order to investigate the optimal fractional order derivative (α) that yields to the best desired beam deflection. Moreover, it has been shown that, for the first natural frequency, the proposed analytical model results in excellent beam deflection results. Nevertheless, for other beam's natural frequencies, validations of the proposed analytical model could be performed. Moreover, the impact of various mass ratios between the moving load and the total weight of the beam could be held in future studies. Additionally, the problem can be improved for moving vehicles, trains, or multiloads or masses, and the effect of the functionally graded material on the dynamic response may also be studied. Furthermore, the effect of large deformations on the beam dynamic deflection can be studied, where a nonlinear term is to be added to the beam governing equation, and in this particular case, approximate numerical solutions are expected to be generated.

Data Availability

The data that support the findings of the study are available from the corresponding author upon request.

Conflicts of Interest

The authors declare that they have no conflicts of interest.

References

[1] Y. A. Rossikhin, M. V. Shitikova, and M. G. E. Meza, "Modeling of the impact response of a beam in a viscoelastic medium," *Applied Mathematical Sciences*, vol. 10, no. 49, pp. 2471–2481, 2016.

[2] S. Paunović, M. Cajić, D. Karličić, and M. Mijalković, "A novel approach for vibration ´ analysis of fractional viscoelastic beams with attached masses and base excitation," *Journal of Sound and Vibration*, vol. 463, Article ID 114955, 2019.

[3] M. Klanner, M. S. Prem, and K. Ellermann, "Steady-state harmonic vibrations of viscoelastic Timoshenko beams with fractional derivative damping models," *Applied Mechanics*, vol. 2, no. 4, pp. 797–819, 2021.

[4] M. Hilal and H. S. Zibdeh, "Vibration analysis of beams with general boundary conditions transversed by a moving force," *Journal of Sound and Vibration*, vol. 229, no. 2, pp. 377–388, 2000.

[5] W. Sumelka, T. Blaszczyk, and C. Liebold, "Fractional Euler-Bernoulli beams: theory, numerical study and experimental validation," *European Journal of Mechanics A: Solids*, vol. 54, pp. 243–251, 2015.

[6] T. Blaszczyk, "Analytical and numerical solution of the fractional Euler–Bernoulli beam equation," *Journal of Mechanics of Materials and Structures*, vol. 12, no. 1, pp. 23–34, 2017.

[7] R. L. Bagley and P. J. Torvik, "Fractional calculus-a different approach to the analysis of viscoelastically damped structures," *AIAA Journal*, vol. 21, no. 5, pp. 741–748, 1983.

[8] I. Podlubny, *Fractional Differential Equations*, Academic Press, San Diego, CA, USA, 1999.

[9] W. Flügge, *Viscoelasticity*, Blaisdell Publishing Company, Massachusetts, MA, USA, 1st edition, 1967.

[10] A. Pipkin, "Lectures on viscoelasticity theory," *Applied Mathematical Sciences*, Springer-Verlag, New York, NY, USA, 1972.

[11] R. M. Christensen, *Theory of Viscoelasticity an Introduction*, Academic Press, New York, NY, USA, 1982.

[12] M. Di Paola, G. Failla, and A. Pirrotta, "Stationary and non-stationary stochastic response of linear fractional viscoelastic systems," *Probabilistic Engineering Mechanics*, vol. 28, pp. 85–90, 2012.

[13] K. Adolfsson, "Non-linear fractional order viscoelasticity at large strains," *Nonlinear Dynamics*, vol. 38, no. 1-4, pp. 233–246, 2004.

[14] A. Ouzizi, F. Abdoun, and L. Azrar, "Dynamic analysis of beams on fractional viscoelastic foundation subject to a variable speed moving load," *MATEC Web of Conferences*, vol. 286, Article ID 01006, 2019a.

[15] A. Ouzizi, H. Bakhti, F. Abdoun, and L. Azrar, "Dynamic analysis of beams on fractional viscoelastic foundation subject to a multiple harmonic moving loads," in *Proceeding 4th World Conference on Complex Systems (WCCS)*, Ouarzazate, Mo, USA, August 2019.

[16] R. K. Praharaj and N. Datta, "Dynamic response of Euler–Bernoulli beam resting on fractionally damped viscoelastic foundation subjected to a moving point load," *Proceedings of the Institution of Mechanical Engineers Part C: Journal of Mechanical Engineering Science*, vol. 234, no. 24, pp. 4801–4812, 2020.

[17] R. Jena, S. Chakraverty, and S. Jena, "Dynamic response analysis of fractionally damped beams subjected to external loads using Homotopy Analysis Method (HAM)," *Journal of Applied and Computational Mechanics*, vol. 5, no. 2, pp. 355–366, 2019.

[18] Z. Liang and X. Tang, "Analytical solution of fractionally damped beam by Adomian decomposition method," *Applied Mathematics and Mechanics*, vol. 28, no. 2, pp. 219–228, 2007.

[19] C. Svedholm, A. Zangeneh, C. Pacoste, S. François, and R. Karoumi, "Vibration of damped uniform beams with general end conditions under moving loads," *Engineering Structures*, vol. 126, pp. 40–52, 2016.

[20] P. Łabędzki, R. Pawlikowski, and A. Radowicz, "Transverse vibration of a cantilever beam under base excitation using fractional rheological model," *AIP Conference Proceedings*, vol. 2029, Article ID 020034, 2018.

[21] T. Blaszczyk, J. Siedlecki, and H. G. Sun, "An exact solution of fractional Euler-Bernoulli equation for a beam with fixed-supported and fixed-free ends," *Applied Mathematics and Computation*, vol. 396, Article ID 125932, 2021.

[22] K. A. Abro, A. Atangana, and A. R. Khoso, "Dynamical behavior of fractionalized simply supported beam: an application of fractional operators to Bernoulli-Euler theory," *Nonlinear Engineering*, vol. 10, no. 1, pp. 231–239, 2021.

[23] I. M. Abu-Alshaikh, A. N. Al-Rabadi, and H. S. Alkhaldi, "Dynamic response of beam with multi-attached oscillators and moving mass: fractional calculus approach," *Jordan Journal of Mechanical and Industrial Engineering*, vol. 8, pp. 275–288, 2014.

[24] Maplesoft, ***Maple*** *Waterloo*, A division of Waterloo Maple Inc, Ontario, Canada, 2019.

[25] T. D. Shermergor, "On the use of fractional differentiation operators for the description of elastic aftereffect properties of materials," *Journal of Applied Mechanics and Technical Physics*, vol. 7, no. 6, pp. 85–87, 1971.

[26] Y. A. Rossikhin and M. V. Shitikova, "Fractional operator models of viscoelasticity," in *Encyclopedia of Continuum Mechanics*, H. Altenbach and A. Öchsner, Eds., Springer, Berlin, Heidelberg, 2020.

[27] A. Nasir, *Response of Fractionally Damped Beams with Appendages Subjected to a Moving Mass*, Springer, Berlin, Heidelberg, 2017.

[28] A. Bonfanti, J. L. Kaplan, G. Charras, and A. Kabla, "Fractional viscoelastic models for power-law materials," *Soft Matter*, vol. 16, no. 26, pp. 6002–6020, 2020.

[29] S. Di Lorenzo, M. Di Paola, F. Pinnola, and A. Pirrotta, "Stochastic response of fractionally damped beams," *Probabilistic Engineering Mechanics*, vol. 35, pp. 37–43, 2014.

[30] S. Rao, *Mechanical Vibrations*, Pearson Prentice Hall, Hoboken, NY, USA, 5th edition, 2011.

[31] R. Abu-Mallouh, I. Abu-Alshaikh, H. S. Zibdeh, and K. Ramadan, "Response of fractionally damped beams with general boundary conditions subjected to moving loads," *Shock and Vibration*, vol. 19, no. 3, pp. 333–347, 2012.

[32] M. Kwong, C. S. Leung, and T. Harko, "A brief introduction to the Adomian decomposition method, with applications in astronomy and astrophysics," 2021.

[33] M. A. Foda and Z. Abduljabbar, "A dynamic green function formulation for the response of a beam structure to a moving mass," *Journal of Sound and Vibration*, vol. 210, no. 3, pp. 295–306, 1998.

[34] L. Fryba, *Vibration of Solids and Structures under Moving Loads*, Noordhoff International Publishing, Groningen, Netherlands, 1972.

[35] J. Freundlich, "Dynamic response of a simply supported viscoelastic beam of a fractional derivative type to a moving force load," *Journal of Theoretical and Applied Mechanics*, vol. 54, pp. 1433–1445, 2016.